J. Phys.: Condens. Matter **20** (2008) 104209 (7pp) doi:10.1088/0953-8984/20/10/104209

Plasticization effect of C_{60} on the fast dynamics of polystyrene and related polymers: an incoherent neutron scattering study

Alejandro Sanz[1], Markus Ruppel[1], Jack F Douglas[2] and João T Cabral[1,3]

[1] Department of Chemical Engineering, Imperial College, London SW7 2AZ, UK
[2] Polymers Division, NIST, Gaithersburg, MD 20899, USA

E-mail: j.cabral@imperial.ac.uk

Received 24 July 2007, in final form 27 November 2007
Published 19 February 2008
Online at stacks.iop.org/JPhysCM/20/104209

Abstract

We utilize inelastic incoherent neutron scattering (INS) to quantify how fullerenes affect the 'fast' molecular dynamics of a family of polystyrene related macromolecules. In particular, we prepared bulk nanocomposites of (hydrogenous and ring-deuterated) polystyrene and poly(4-methyl styrene) using a rapid precipitation method where the C_{60} relative mass fraction ranged from 0% to 4%. Elastic window scan measurements, using a high resolution (0.9 μeV) backscattering spectrometer, are reported over a wide temperature range (2–450 K). Apparent Debye–Waller (DW) factors $\langle u^2 \rangle$, characterizing the mean-square amplitude of proton displacements, are determined as a function of temperature, T. We find that the addition of C_{60} to these polymers leads to a progressive increase in $\langle u^2 \rangle$ relative to the pure polymer value over the entire temperature range investigated, where the effect is larger for larger nanoparticle concentration. This general trend seems to indicate that the C_{60} nanoparticles *plasticize* the fast ($\approx 10^{-15}$ s) local (≈ 1 Å) dynamics of these polymer glasses. Generally, we expect nanoparticle additives to affect polymer dynamics in a similar fashion to thin films in the sense that the high interfacial area may cause both a speeding up and slowing down of the glass state dynamics depending on the polymer–surface interaction.

1. Introduction

Numerous recent studies [1] have focused on changes in the dynamics of nanoscale confined polymers because of the many technological implications for nanotechnology in materials design, development, and processing. Further, such studies have the potential of elucidating fundamental aspects of glass formation. Most studies of confined polymers have emphasized the dependence of the glass transition temperature T_g on thin film thickness L [1, 2], where dramatic reductions of T_g with decreasing L (when L is less than a monomer dependent packing scale typically on the order of O(100 nm)) have been reported in both supported and free-standing films of polystyrene and other relatively 'fragile' glass-forming polymers [1]. Moreover, studies reporting T_g as a function of distance from the film surfaces suggest the existence of mobility gradients in thin polymer films [1–4]. The problem with these estimates, from our standpoint, is that the physical meaning of T_g is even uncertain from a fundamental perspective in the bulk, so the significance of reported T_g 'shifts' as means of quantifying the mobility changes arising from film confinement is unclear. Further, different experimental methods on the same film seem to give different apparent T_g shift estimates [5–10], so it is not even clear whether film T_g determinations are internally consistent phenomenologically. Given these difficulties, and the practical importance of the problem, we are concerned with developing more reliable metrics for describing mobility changes in confined polymers with nanoparticle additives.

[3] Author to whom any correspondence should be addressed.

Inelastic incoherent neutron scattering (INS) provides a promising approach to this problem because it allows for a direct measurement of local mobility (proton self-correlation function) and this method has been recently employed to probe the dynamics of ultrathin polymer films [5–11] (films having a thickness comparable to molecular dimensions, where chain packing becomes modified). Specifically, stacked polymer thin films were studied in pioneering backscattering measurements, which allowed for the determination of an apparent Debye–Waller (DW) factor, $\langle u^2 \rangle$. These measurements indicated hindered proton motion for supported films upon confinement, while a reverse trend has been reported for 'free-standing' ultrathin films [5–11] ('free-standing' films, however, are inherently under highly non-equilibrium conditions, since they are not thermally annealed). Inoue and co-workers [12] have recently investigated glassy supported PS thin films by quasielastic neutron scattering (QENS), in combination with INS, where a general suppression in the amplitude of molecular motion with confinement was indicated by *both* $\langle u^2 \rangle$ and boson peak measurements, in good qualitative accord with earlier observations by Soles and co-workers on polycarbonate and other polymers [5–10]. A suppression of the average mean-square particle displacement has also been recently found in low energy collisional transfer measurements on thin PMMA films, where helium atoms rather than neutrons are involved in the scattering measurement [13]. Other authors have observed a general tendency for the thermal expansion to become reduced in thin polymer films [5–10, 14–17], and a general tendency for a broadening of the temperature range over which the glass transition occurs [18, 19].

The present work extends dynamic neutron scattering investigation (INS) to polymer nanocomposites, which are likewise characterized physically by a high interfacial area and where large changes in polymer dynamics relative to pure bulk materials have been reported. Indeed, recent experimental studies have indicated that the changes in the apparent T_g for dispersions of nanoparticles exhibit similar trends to those found in ultrathin polymer films [20], and arguments have been put forth to support this correspondence [20–23]. It has also been observed that the addition of certain molecular additives to a polymer matrix can lead to a reduction of the effects of spatial confinement on the T_g of thin (polystyrene) films [24]. Simulations [25, 26] have shown that this effect can be understood to arise from a decrease of the length scale of cooperative segmental motion that arises from the effect of 'anti-plasticizing' additives on molecular packing. Such additives characteristically result in an increase of polymer density and shear modulus in the glass state while, at the same time, shifting T_g downwards. Simulations suggest that both film confinement and the addition of anti-plasticizers make glass formation 'stronger' [25, 26], meaning that the glass transition covers a larger temperature range (becomes broader) and that deviations from the Arrhenius temperature dependence, characteristic of simple homogeneous fluids, becomes weaker. The 'nature' of glass formation appears to be altered by confinement or the presence of anti-plasticizing additives. It is thus clear that the determination of T_g alone seems therefore inadequate to characterize mobility changes arising from geometrical confinement or additives.

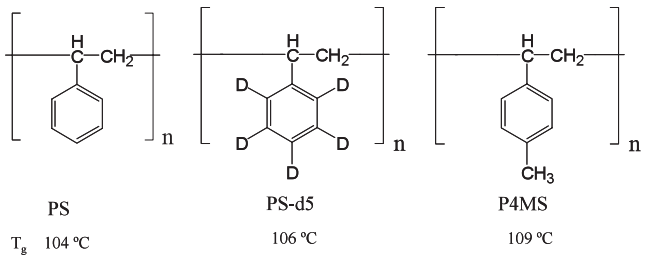

Figure 1. Monomer structures of poly(styrene), ring-deuterated polystyrene and poly(4-methyl styrene) with corresponding glass transition temperatures T_g.

Here we present an experimental study of the influence of well dispersed nanoparticles on the glassy dynamics of a family of PS materials. We selected fullerenes (C_{60}) because of their well defined chemical nature and monodisperse particle size and we chose a family of PS polymers in order to elucidate the interplay between the molecular geometry of the nanoparticle and the polymer matrix to which it is added. We consider fixed window elastic scans on a high resolution backscattering spectrometer and determine the apparent mean-square proton displacement $\langle u^2 \rangle$, the so-called Debye–Waller factor, for PS/C_{60} nanocomposites as a function of temperature.

2. Experimental details

2.1. Sample preparation[4]

C_{60} nanocomposites with PS were prepared using a rapid precipitation method [27, 28]. The fullerene (Mer Corporation, AZ, exceeding 99% purity) material was used as received. Polystyrene (PS), ring-deuterated polystyrene (PS-d5, deuteration in excess of 95%) and poly(4-methyl styrene) (P4MS) were selected as polymer matrices. PS (BP Chemicals, molecular mass, $M_w = 225$ kg mol^{-1}, polydispersity index, PDI = 2.2) and P4MS (Aldrich, $M_w = 73$ kg mol^{-1}, PDI = 1.8) were re-precipitated in fivefold excess of methanol to remove low molecular weight stabilizers. PS-d5 was synthesized via hydrogen–deuterium exchange of the phenyl ring by a catalytic reaction in the presence of ethylaluminium dichloride (1.0 M solution in hexanes, Aldrich) and traces of water from hydrogenous PS as starting material [29]. The chemical structures of the repeat units and the corresponding T_g values of the polymers are depicted in figure 1.

The C_{60} nanoparticles were dissolved in toluene and placed in an ultrasonic bath (Transsonic T570/H, Camlab, freq = 50/60 Hz; $I = 1.5$ A, HF-freq = 35 kHz) for 30 min to facilitate particle dispersion. The corresponding amount of polymer was then added to the solution to obtain the desired concentration of C_{60} in the polymer matrix, keeping a 10% relative mass fraction of the mixture polymer/C_{60} in toluene. The polymer/C_{60} toluene solution was further sonicated for 30 min. The mixture was stirred for 48 h at room temperature

[4] Certain equipment, instruments or materials are identified in this paper in order to adequately specify the experimental details. Such identification does not imply recommendation by the NIST nor does it imply the materials are necessarily the best available for the purpose.

and then precipitated in a fivefold volume excess of methanol to produce composite fibres. The precipitated samples were dried under vacuum at 90 °C for 4 days. PS/C_{60} specimens were extruded into 1 mm diameter fibres (as suggested by Mackay *et al* [27]) using a DSM microextruder operating at 170–180 °C and 150 rpm (1 rpm $= 2\pi$ rad min^{-1}); P4MS and PS-d5 specimens were not microextruded due to limited sample mass. Specimens were then melt pressed at 150 °C for 5 min and subsequently quenched to room temperature. The film thicknesses were selected to provide a neutron transmission of 90% to 95%, achieved with 170–200 μm films. The scattering signal is largely dominated by the incoherent cross-section of hydrogen and selective deuteration is employed to elucidate different parts of the monomer unit.

2.2. Inelastic incoherent neutron scattering

Inelastic incoherent neutron scattering experiments were carried out at the backscattering spectrometer IN16, at the *Institut Laue Langevin*, France. The configuration selected provides 0.9 μeV resolution (FWHH, full width at half height), energy window $-15 \leqslant \Delta E \leqslant 15$ μeV, and wavenumber range $0.2 \leqslant Q \leqslant 1.9$ Å^{-1}, where $Q = 4\pi \sin(\theta/2)/\lambda$, θ is the scattering angle and λ the neutron wavelength (6.27 Å). Both fixed window scans ($\Delta E \approx 0$) and inelastic spectra were measured, although only the former will be discussed in this report, centred on the Debye–Waller (DW) dynamics. Elastic (or fixed window) scans covered a typical temperature range of 2 K $< T <$ 450 K, accessible with a cryofurnace, and lasted for typically 9–14 h (depending on scattering cross-section). These measurements monitor the evolution of the elastic scattering intensity as a function of temperature and momentum transfer Q, and provide a direct measure of the DW factor below the onset of side-group or segmental motion in glassy polymers [30, 31].

The measured elastic scattering intensity $S_{\rm inc}(Q, \omega \approx 0)$ is a convolution of the dynamic structure factor $S_{\rm inc}(Q, \omega)$ with the experimental resolution $R(\omega)$:

$$S_{\rm elastic}(Q) \equiv S_{\rm inc}(Q, \omega \approx 0) = \int_{-\infty}^{+\infty} S_{\rm inc}(Q, \omega') R(\omega - \omega')\, {\rm d}\omega \Big|_{\omega=0}, \quad (1)$$

which assumes that no rotational ($S_{\rm rot} = 1$) or translational ($S_{\rm trans} = 1$) motions are present. Equation (1) at constant temperature T becomes simply the Debye–Waller factor,

$$S_{\rm elastic}(Q) \approx \exp(-Q^2\langle u^2\rangle/3) \quad (2)$$

where $\langle u^2\rangle$ is the mean-square amplitude of proton vibrations. The assumption is valid provided that the temperature is sufficiently low to 'freeze' side-group or segmental dynamics (i.e. appear immobile at given resolution) and that the centre of mass of the molecule is fixed (below $T_{\rm g}$). In practice, during a window scan experiment, an 'apparent' Debye–Waller factor $\langle u^2\rangle_{\rm app}(T)$ is measured as a function of temperature (2–450 K in the present work), and proton vibrations $\langle u^2\rangle$ are estimated from an extrapolation using the low temperature range. For harmonic atomic vibrations [30, 32], a linear dependence of $\ln(I_{\rm elastic})$ versus Q^2 is expected, from which it is possible to estimate the mean proton displacement $\langle u^2\rangle$. Deviations from this linearity indicate anharmonic modes, as well as the onset of other kinds of motion such as librations, rotations, secondary relaxations, etc. The analysis of the rotational relaxation in this PS family will be reported in a subsequent publication.

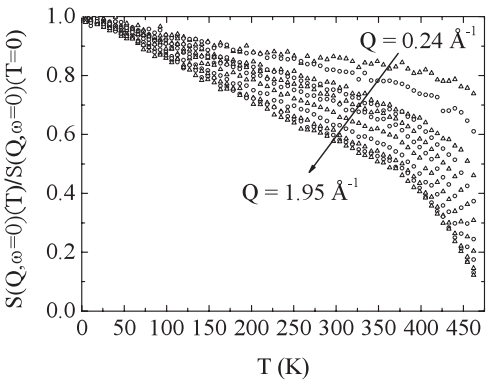

Figure 2. Fixed window scan (at 0.9 μeV resolution) of poly(styrene) from T equal to 2–470 K, at selected wavenumbers Q ranging from 0.24 to 1.95 Å^{-1} (from top to bottom). The results are normalized by the elastic intensity extrapolated to 0 K.

3. Results and discussion

The elastic neutron intensity of neat PS, normalized to the extrapolated intensity at $T = 0$ K, as a function of temperature at different Q values is shown in figure 2. Measurement uncertainty determined by neutron counting statistics (9–14 h acquisitions) is ≈2%, which is smaller than the size of symbols in figures 2–4. At T below ≈75 K, the decrease in elastic intensity is solely due to the DW factor. In other words, the dynamics is purely vibrational and the mean-square displacement can be readily estimated. Beyond this temperature range, the steeper drop in the elastic intensity indicates the onset of larger scale motions, such as the reorientation of the phenyl ring. At higher temperatures, near 100 °C, the onset of the glass transition is indicated by a dramatic decrease of the elastic intensity. The mean-square displacement $\langle u^2\rangle$ at various T was computed according to equation (2). Figure 3 shows the experimental data of $\ln(I_{\rm elastic})$ versus Q^2 and the corresponding linear fits, whose slope is $-\langle u^2\rangle_{\rm app}/3$, for neat PS at different temperatures below and above $T_{\rm g}$. The deviations from linearity, especially at higher temperatures, can be originated by the anharmonicity of the motions and onset of larger scale dynamics, as well as by the contribution of the coherent scattering to the elastic intensity [30–32].

The goal of this work is to investigate the qualitative influence of C_{60} ('buckyballs') on the local proton dynamics of PS and related polymers in the glassy state. Figure 4 presents fixed window scans of neat PS and PS/C_{60} nanocomposites (relative mass fractions: 2.0% and 4.0%) at $Q = 1.91$ Å^{-1}. There are no obvious differences between PS and nanocomposites in this representation, becoming clearer when data for all Q are summed in figure 4(b). A more

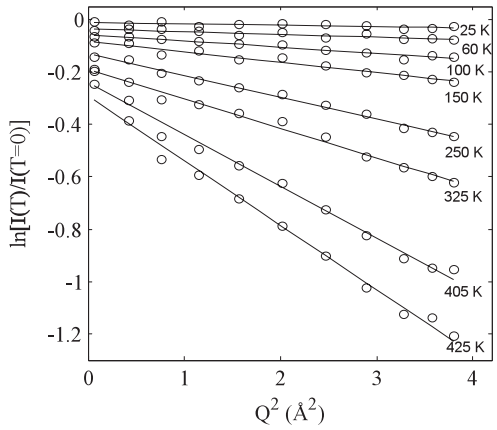

Figure 3. Logarithm of the normalized elastic intensity of PS as a function of Q^2 for selected temperatures to extract the *apparent* Debye–Waller factor. Identifying the slope $-\langle u^2\rangle/3$ provides an estimate of the mean-square displacement.

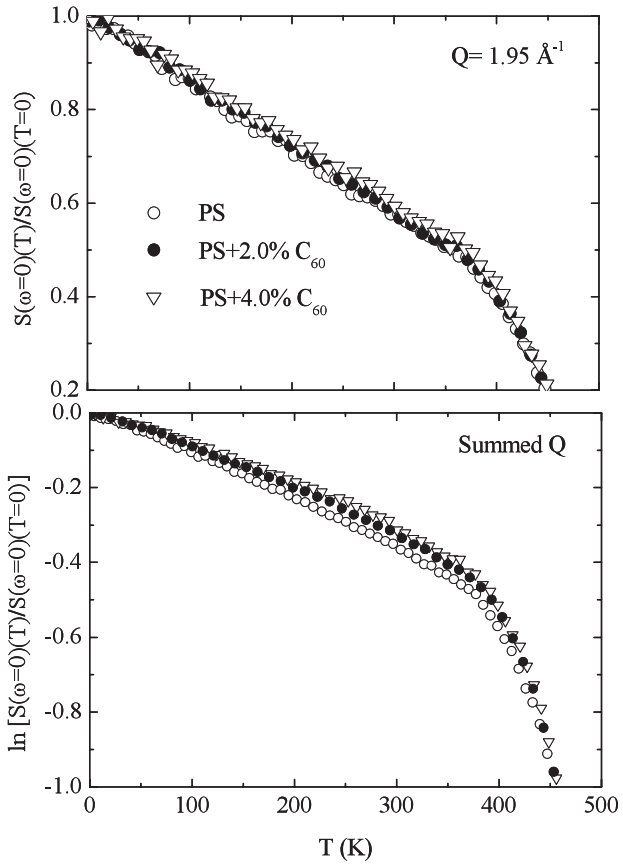

Figure 4. (a) Elastic scan of poly(styrene) with C_{60} filler concentrations ranging from 0% to 4% relative mass fraction as a function of temperature for a fixed wavenumber, $Q = 1.95$ Å^{-1}. (b) Elastic scan summed at all wavenumbers Q for selected PS specimens with C_{60} mass fractions: 0%, 2% and 4%.

direct comparison is obtained by estimating $\langle u^2\rangle$ as a function of temperature. Figure 5 indicates small but measurable differences between the neat PS when compared to the PS/C_{60} nanocomposites. Below T_g, the proton displacement amplitude

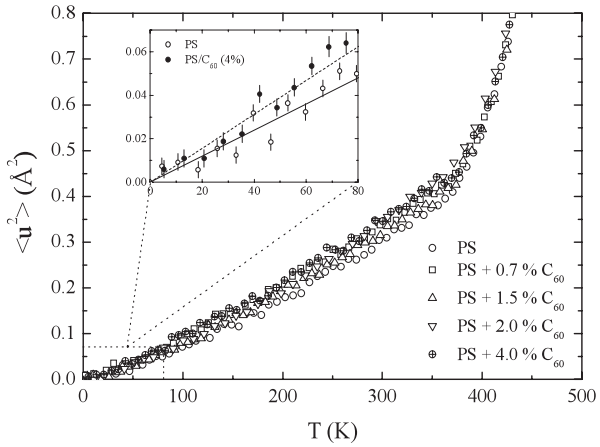

Figure 5. Apparent mean-square displacement $\langle u^2\rangle$ (Å^2) as a function of temperature for neat and filled polystyrene. The inset shows the low temperature range (below the onset of rotational relaxation and segmental dynamics) of PS and a PS nanocomposite with a 4% C_{60} mass fraction. An enhanced amplitude of motion with dilution by C_{60} is evident.

is somewhat larger for PS/C_{60} composites and we contrast data for PS and PS/C_{60} (4% C_{60} mass fraction) samples in the low temperature region in the inset of figure 5 (only 4% is shown for clarity). Typical $\langle u^2\rangle$ uncertainty estimated from the extrapolation in figure 3 is 4×10^{-3} Å^2. We observe that the PS/C_{60} samples exhibit a steeper slope of $\langle u^2\rangle$ with temperature, as compared to the neat PS. We quantify these changes by fitting a linear function of T over the relevant temperature range (0–80 K) to obtain the slope $m = \mathrm{d}\langle u^2\rangle/\mathrm{d}T$, where '%' in the following denotes the relative C_{60} mass fraction: m(PS) $= (6.0 \pm 0.3) \times 10^{-4}$ Å^2 K^{-1}, m(PS; 0.7%) $= (7.7 \pm 0.5) \times 10^{-4}$ Å^2 K^{-1}, m(PS; 1.5%) $= (6.2 \pm 0.5) \times 10^{-4}$ Å^2 K^{-1}, m(PS; 2%) $= (7.0 \pm 0.5) \times 10^{-4}$ Å^2 K^{-1}, and m(PS; 4%) $= (7.8 \pm 0.3) \times 10^{-4}$ Å^2 K^{-1}. The relative uncertainties were computed by averaging estimates obtained between 0–50 and 0–80 K and determining the maximum range of m found. We suggest that the comparatively large value obtained for the 0.7% C_{60} mass fraction sample (similar to the 4% mass fraction specimen) could be due to concentration non-uniformities in the microextruded nanocomposites fibres (due to small sample mass, ≈1–2 g). Nevertheless, all the samples indicated a stronger temperature dependence of $\langle u^2\rangle$ with the addition of C_{60}.

According to the idealized harmonic solid model, the slope of the dependence of $\langle u^2\rangle$ on temperature is related to the effective local 'stiffness' [25, 26, 30, 33] of the material by means of the relation

$$\kappa = 3k_B T/\langle u^2\rangle, \tag{3}$$

where k_B is Boltzmann's constant. The application of equation (3) outside the low temperature regime ($T \geqslant 80$ K) is clearly heuristic since the harmonic approximation is strictly not applicable at elevated temperatures [25, 26, 30] and other activated processes (side-group rotations and backbone

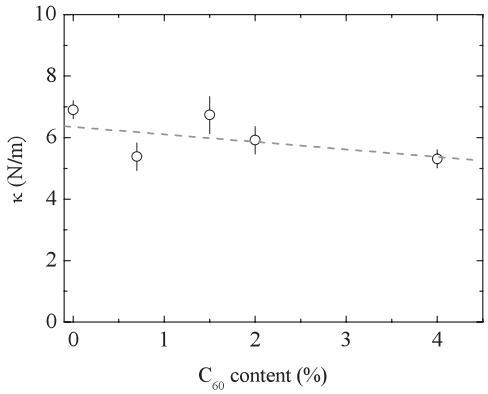

Figure 6. Harmonic force constant κ as a function of C_{60} additive concentration; the dashed line serves as a guide to the eye.

motion) dominate the loss of elastic intensity [30, 31]. Figure 6 shows the evolution of the apparent force constant κ versus C_{60} content, where we see an overall decrease of κ for PS/C_{60} nanocomposites in comparison with the neat PS. Uncertainties in κ are obtained by error propagation of $\langle u^2 \rangle$ according to equation (3).

In order to discriminate between the dynamics of the backbone and phenyl ring protons, and how they are modified by the nanoparticle additives, we also investigated a ring-deuterated derivative of PS, which we designate as PS-d5. The apparent DW factor $\langle u^2 \rangle$ for the neat PS-d5 and the C_{60} nanocomposite (0.5% C_{60} mass fraction) polymer matrix is presented in figure 7(a). P4MS has a methyl group attached to the 4-phenyl site and is considerably brittle compared to PS. Figure 7(b) presents DW measurements for the derivative polymer P4MS, as well as for the C_{60} nanocomposite (0.5% C_{60} mass fraction). In both cases, we observe a clear increase in the apparent DW factor with the addition of C_{60}. A detailed account of contributions from localized rotational relaxations (methyl and phenyl group dynamics, namely mean activation energy E_A and distribution σ) is beyond the scope of the present paper and will be discussed in a separate paper [34]. Due to the very low activation energy of the methyl group rotational relaxation in P4MS, it is extremely difficult to quantify the DW factor by low temperature extrapolation. However, the window scan measurements indicate a larger apparent mean-square displacement, corresponding to enhanced motion in the glassy state. The slope m describing the strength of the temperature dependence of $\langle u^2 \rangle$ in PS-d5/C_{60} (0.5% C_{60} mass fraction), where the scattering is largely dominated by the backbone protons, appears to increase by almost one order of magnitude with respect to hydrogenous PS. We obtain $m(\text{PS-d5/C}_{60}) = (4.5 \pm 0.5) \times 10^{-4}$ Å^2 K^{-1} and $m(\text{PS-d5}) = (6.5 \pm 1.5) \times 10^{-5}$ Å^2 K^{-1} (uncertainties estimated as indicated above). We conclude from all our measurements that the addition of small amounts of C_{60} to the PS polymer derivatives (PS, PS-d5 and P4MS) generally enhances the fast glassy dynamics, as measured by the proton delocalization in the femtosecond time range [30, 31].

The harmonic solid model provides a qualitative framework for interpreting these results. Figure 6 suggests

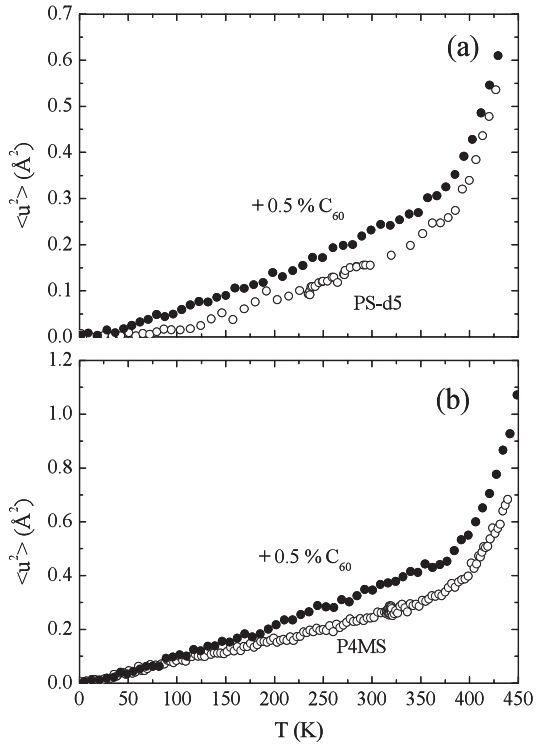

Figure 7. Apparent mean-square displacement $\langle u^2 \rangle$ (Å^2) as a function of temperature for neat (a) ring-deuterated PS (PS-d5) and (b) poly(4-methyl styrene) (P4MS) and filled with 0.5% relative mass fraction of C_{60} nanoparticles.

that the C_{60} nanoparticles induce a *softening* of the local potential which reduces the resistance to displacement of the protons of the polymer segments. This 'plasticization' effect is corroborated by plots of figure 7, where a clear increase of $\langle u^2 \rangle$ for the whole temperature range is observed. We suggest that the physical origin of this enhancement of amplitude of molecular motion of PS and its derivatives in the glassy state is caused by an increased free volume arising from an enhanced packing frustration obtained by introducing the marginally soluble C_{60} nanoparticles into the melt of this class of polymers. The opposite effect of a slowing down of the amplitude of molecular motions with nanoparticles has been previously associated [21–23, 35] with the development of strong specific associations between the polymer and particle. The addition of nanoparticles to polymers is thus expected to have non-universal effects in polymer dynamics, depending on interactions between the polymer and the particle, and both plasticization and anti-plasticization might occur. A recent INS report on C_{60} dispersed in poly(methyl methacrylate) suggested reduced mobility of polymer chains in the presence of the additive [36], attributed to strong interactions between PMMA and C_{60}. Mean square displacement estimates are not provided, likely because DW factors cannot be accurately estimated from elastic window scans *above* temperatures of 50 K in the presence of side-group motion. Nevertheless, higher temperature rotational relaxations appear to be affected by the presence of particles and a restriction of dynamics (and greater dynamic heterogeneity) is suggested. Figure 9 from

Kropka *et al* [36] can be compared directly to our figure 4(b), where elastic temperature data is summed at all wavenumbers, and suggests a similar trend for *rotational/segmental motion* in PS/C_{60} and PMMA/C_{60} systems. These complementary observations for the PS class of polymers and PMMA suggest that polymer–particle interactions, as quantified by solvent quality effects, might be able to inform us about the change in polymer dynamics with these additives at the various relevant time- and length scales.

A consideration of how the chain dimensions change with the addition of additives provides a traditional way to quantify these polymer–additive interactions. Based on their small angle neutron scattering measurements on C_{60} filled PS, Mackay *et al* [27] have proposed that chains become expanded in the presence of C_{60} particles at low C_{60} content so that these particles then behave like a 'good' solvent. These results corroborate earlier observations by Nakatani *et al* [37, 38] on poly(dimethyl siloxane) using cross-linked PDMS nanoparticle additives of various sizes. Nakatani *et al* suggested that sufficiently small particles (diameter below the polymer's radius of gyration, R_g) could cause substantial chain expansion at relatively low particle concentrations, while particle aggregation seems to become prevalent at high particle concentrations. A systematic study of these solvent quality effects might be helpful in predicting changes in molecular dynamics in polymer–diluent systems and we plan to investigate this matter in the future.

Plasticization and anti-plasticization of polymers can occur with a variety of additives [39–52]. Here we have centred specifically on fast ($\approx 10^{15}$ Hz) proton delocalization in the glassy state. Based on this work, we conclude that C_{60} generally increases the amplitude of molecular motion in PS and related polymers, meaning that C_{60} *plasticizes* [39] these polymers. Our results are thus qualitatively similar to previous observations on the addition of $CaCO_3$ nanoparticles to poly(4-methyl-2-pentyne) films [53], where the nanoparticles were found to give rise to an *increase* in the free volume of the polymer melt (as measured in these measurements by positron annihilation), as well as a corresponding increase in gas permeability. We likewise attribute the changes we observe to an increase in molecular 'free volume', as quantified precisely here by $\langle u^2 \rangle$ [21–23], that arises from the disruption of molecular packing brought about by the addition of the C_{60} nanoparticles. This effect is *opposite* to the case of anti-plasticizer additives, which reduce the molecular free volume [25, 26]. Moreover, recent measurements [15, 16, 54] by a variety of methods (INS, dielectric, mechanical) have indicated that additives can act as both plasticizers and anti-plasticizers, depending on the temperature range investigated. While many additives anti-plasticize at low temperatures well below T_g and plasticize at temperatures higher than T_g, other additives exhibit the inversion of this trend [15, 16, 54]. Further work is required to establish the effect of the addition of nanoparticles to polymers, with due consideration of specific interactions and mixture thermodynamics, both in terms of chain and glass structure and various dynamical processes present in polymers.

4. Conclusions

We present the first experimental study of mean-square displacement of protons in a family of model polystyrenes in the presence of C_{60} nanoparticles, using high resolution backscattering. Fixed window scans of filled PS at various C_{60} concentrations, covering a wide temperature range, was presented. Additionally, we vary the contrast (PS-d5) and monomer architecture (P4MS) and study both the neat and filled polymers (0.5% C_{60} relative mass fraction). Our experimental results generally indicate that the addition of C_{60} to PS leads to enhanced fast dynamics (as measured by the mean-square amplitude of proton displacements) consistent with C_{60} plasticizing PS much like the addition of a typical small molecule solvent to the polymer melt. This effect is not obvious and slowing down of the polymer melt fast dynamics is also expected by tuning polymer–particle interactions. The addition of nanoparticles thus provides an attractive approach for modifying the properties of polymer materials through a modulation of molecular packing, and elastic neutron scattering seems to be a powerful tool for quantifying these changes in molecular dynamics that accompany dilution and confinement. A detailed study of specific rotational relaxation motions (methyl and phenyl rotations) in our model filled polymers is currently underway.

Acknowledgments

We gratefully acknowledge the *Institut Laue Langevin* (ILL) Grenoble, France, for beamtime, *ISIS*, Oxfordshire, UK, for support and Lambert Van Eijck for assistance during the experiment. AS thanks the Spanish Ministry of Science and Education (*Ministerio de Educación y Ciencia*) for a post-doctoral fellowship. JFD thanks Chris Soles of NIST for useful conversations relating to inelastic incoherent neutron scattering.

References

[1] Alcoutlabi M and McKenna G B 2005 *J. Phys.: Condens. Matter* **17** R461
[2] Keddie J L, Jones R A L and Cory R A 1994 *Europhys. Lett.* **27** 59
[3] Forrest J A and Dalnoki-Veress K 2001 *Adv. Colloid Interface Sci.* **94** 167
[4] Ellison C J and Torkelson J M 2003 *Nat. Mater.* **2** 695
[5] Soles C L, Lin E K, Lenhart J L, Jones R L, Wu W L, Goldfarb D L and Angelopoulos M 2001 *J. Vac. Sci. Technol.* B **19** 2690
[6] Soles C L 2002 *Phys. Rev. Lett.* **88** 037401
[7] Soles C L, Douglas J F, Lin E K, Lenhart J L, Jones R L and Wu W L 2003 *J. Appl. Phys.* **93** 1978
[8] Soles C L, Douglas J F, Wu W L and Dimeo R M 2003 *Macromolecules* **36** 373
[9] Soles C L, Douglas J F and Wu W L 2004 *J. Polym. Sci.* B **42** 3218
[10] Soles C L 2004 *Macromolecules* **37** 2890
[11] Frick B, Dalnoki-Veress K, Forrest J A, Dutcher J, Murray C and Higgins A 2003 *Eur. Phys. J.* E **12** S93
[12] Inoue R, Kanaya T, Nishida K, Tsukushi I and Shibata K 2005 *Phys. Rev. Lett.* **95** 056102

[13] Freedman M A, Rosenbaum A W and Sibener S J 2007 *Phys. Rev.* B **75** 113410
[14] Orts W J, van Zanten J H, Wu W and Satija S K 1993 *Phys. Rev. Lett.* **71** 867
[15] Miyazaki T, Nishida K and Kanaya T 2004 *Phys. Rev.* E **69** 022801
[16] Miyazaki T, Nishida K and Kanaya T 2004 *Phys. Rev.* E **69** 061803
[17] DeMaggio G B, Frieze W E, Gidley D W, Zhu M, Hristov H A and Yee A F 1997 *Phys. Rev. Lett.* **78** 1524
[18] Kawana S and Jones R A L 2001 *Phys. Rev.* E **6302** 21501
[19] Bhattacharya M, Sanyal M K, Geue T and Pietsch U 2005 *Phys. Rev.* E **71** 041801
[20] Bansal A, Yang H C, Li C Z, Cho K W, Benicewicz B C, Kumar S K and Schadler L S 2005 *Nat. Mater.* **4** 693
[21] Starr F W, Schroder T B and Glotzer S C 2001 *Phys. Rev.* E **6402** 125501
[22] Starr F W, Schroder T B and Glotzer S C 2002 *Macromolecules* **35** 4481
[23] Starr F W, Sastry S, Douglas J F and Glotzer S C 2002 *Phys. Rev. Lett.* **89** 125501
[24] Ellison C J, Ruszkowski R L, Fredin N J and Torkelson J M 2004 *Phys. Rev. Lett.* **92** 095702
[25] Riggleman R A, Yoshimoto K, Douglas J F and de Pablo J J 2006 *Phys. Rev. Lett.* **97** 011504
[26] Riggleman R A, Douglas J F and de Pablo J J 2007 *J. Chem. Phys.* **126** 234903
[27] Mackay M E, Tuteja A, Duxbury P M, Hawker C J, Van Horn B, Guan Z B, Chen G H and Krishnan R S 2006 *Science* **311** 1740
[28] Du F M, Fischer J E and Winey K I 2003 *J. Polym. Sci.* B **41** 3333
[29] Willenberg B 1976 *Makromol. Chem.* **177** 3625
[30] Bee M 1988 *Quasielastic Neutron Scattering* (Bristol: Adam Hilger)
[31] Higgins J S and Benoit H C 1994 *Polymers and Neutron Scattering* (Oxford: Oxford University Press)
[32] Frick B, Buchenau U and Richter D 1995 *Colloid Polym. Sci.* **273** 413
[33] Zaccai G 2000 *Science* **288** 1604
[34] Sanz A, Wong H, Ruppel M and Cabral J T 2008 in preparation
[35] Smith G D, Bedrov D, Li L W and Byutner O 2002 *J. Chem. Phys.* **117** 9478
[36] Kropka J M, Putz K W, Pryamitsyn V, Ganesan V and Green P F 2007 *Macromolecules* **40** 5424
[37] Nakatani A I, Chen W, Schmidt R G, Gordon G V and Han C C 2001 *Polymer* **42** 3713
[38] Nakatani A I, Chen W, Schmidt R G, Gordon G V and Han C C 2002 *Int. J. Thermophys.* **23** 199
[39] Cowie J M G 1998 *Polymers: Chemistry and Physics of Modern Materials* (Cheltenham: Nelson)
[40] Jackson W J and Caldwell J R 1965 *Adv. Chem. Ser.* **48** 185
[41] Jackson W J and Caldwell J R 1967 *J. Appl. Polym. Sci.* **11** 211
[42] Jackson W J and Caldwell J R 1967 *J. Appl. Polym. Sci.* **11** 277
[43] Robeson L M 1969 *Polym. Eng. Sci.* **9** 277
[44] Petrie S E B, Moore R S and Flick J R 1972 *J. Appl. Phys.* **43** 4318
[45] Anderson S L, Grulke E A, Delassus P T, Smith P B, Kocher C W and Landes B G 1995 *Macromolecules* **28** 2944
[46] Maeda Y and Paul D R 1987 *J. Polym. Sci.* B **25** 957
[47] Maeda Y and Paul D R 1987 *J. Polym. Sci.* B **25** 981
[48] Maeda Y and Paul D R 1987 *J. Polym. Sci.* B **25** 1005
[49] Lourdin D, Bizot H and Colonna P 1997 *J. Appl. Polym. Sci.* **63** 1047
[50] Cais R E, Nozomi M, Kawai M and Miyake A 1992 *Macromolecules* **25** 4588
[51] Bergquist P, Zhu Y, Jones A A and Inglefield P T 1999 *Macromolecules* **32** 7925
[52] Anopchenko A, Psurek T, VanderHart D, Douglas J F and Obrzut J 2006 *Phys. Rev.* E **74** 031501
[53] Merkel T C, Freeman B D, Spontak R J, He Z, Pinnau I, Meakin P and Hill A J 2002 *Science* **296** 519
[54] Psurek T, Obrzut J, Soles C L, Page K A, Cicerone M and Douglas J F 2007 submitted